

1. The construction of standard curve for the detection of enzyme activity.

Experiment: 0.15 mol L⁻¹ Tris buffer (pH 8.0) was used to prepare 1.8 × 10⁻⁴ mol L⁻¹ DTNB solution. Then 0.025, 0.050, 0.075, 0.100 and 0.125 mmol L⁻¹ L-cysteine hydrochloride was respectively dissolved in the DTNB solution. After that, the AChE-functionalized 2D-PC was respectively placed into a series of L-cysteine hydrochloride solutions and UV absorbance at 412 nm was monitored.

Table S1 Data of Standard Curve

Concentration of L-cysteine hydrochloride (mmol.L ⁻¹)	Absorbance 1	Absorbance 2	Absorbance 3	Absorbance average
0.025	0.32253	0.3224	0.3225	0.322477
0.050	0.65044	0.65027	0.65001	0.65024
0.075	0.972	0.97182	0.97154	0.971787
0.100	1.26311	1.26312	1.26234	1.262857
0.125	1.59422	1.59169	1.59354	1.59315
0.150	1.89241	1.89133	1.89098	1.891573
0.175	2.21499	2.21065	2.21872	2.214787

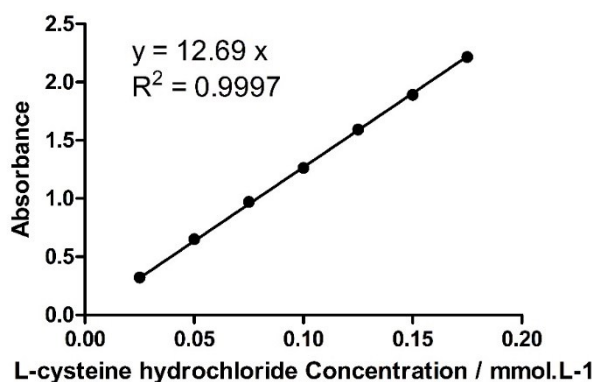


Figure S1 Standard Curve of L-cysteine hydrochloride

2. Measurement of binding amounts of AChE

2.1. Standard curve

Experiment: 2 mL obtained G-250 solution was mixed with 50 μ L AChE solution varied from 0.5 to 3.0 mg/mL (adjusted with 0.15 mol L⁻¹ Tris-HCl buffer, pH=7.4) and UV absorbance at 595 nm was measured.

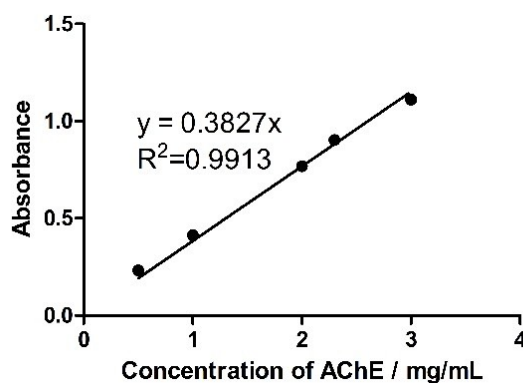


Figure S2 Standard Curve of AChE solution

2.2. Detection of AChE-functionalized 2D-PC

The amount of AChE on film (mg cm^{-2}) meets following equation:

$$m = 4(A_0 - A_1)/(0.25 \times 12K) \quad (S1)$$

where A_0 and A_1 are AChE solution before and after modification respectively, K is the slope of standard curve, 4 is the volume of AChE solution, 0.25 is the area of every film, 12 represents the amount of films.

The change of absorbance ($A_0 - A_1$) and the amounts of AChE on film were depicted in table S2.

Table S2 data of AChE-functionalized 2D-PC

	sample 1	sample 2	sample 3	sample average
Change of absorbance	0.1046	0.1517	0.1131	0.1231
The amounts of AChE on film (mg cm^{-2})	0.36	0.53	0.39	0.43

3. water-solubility of organophosphates

Table S3 Water-solubility of some organophosphates ^a.

organophosphates	dipterex	dichlorvos	malathion	methidathion	acephate	glufosinate-ammonium
water-solubility	soluble	soluble	4.39×10^{-4} mol/L (slightly soluble)	7.94×10^{-4} mol/L (slightly soluble)	soluble	soluble

^a Data sources: <https://www.baidu.com/>

4. Calculations of limit of detection (LOD)

We surmised that there was a linear correlation between particle spacing of our sensor and dipterex concentration at the range of 0~ 10^{-14} mol L⁻¹ before calculations. We measured the responsivity of our AChE-PC sensor to a 50 mL of dipterex at a concentration of 10^{-14} mol L⁻¹ and a 38 nm decrease in particle spacing was observed. The resulting responsivity was calculated as $S=38 \times 10^{14}$ nm/(mol L⁻¹). At the blank solution, the average standard deviation is $\sigma=8.9$ nm. As a consequence, the $LOD=3.3 \times \sigma/S=7.7 \times 10^{-15}$ mol L⁻¹.

5. Performance comparison of different materials

Table S4 Comparison of various analytical methods for sensing Sarin analogs

Method Names	Analyte	Strengths/ Weakness	Sensitivity	References
AChE-functionalized 2D-PC	Dipterex	S: detecting organophosphate with high sensitivity; miniaturized; simple detection device; simple preparation; W: can't detect dipterex in complex environment until now.	LOD: 0.77×10^{-14} mol L ⁻¹	This study
3D-PC biosensor	Sarin	S: detecting a real chemical warfare with high sensitivity;	LOD: 10^{-15} mol L ⁻¹	[1]

		W: can't detect Sarin in complex environment until now.	
SERS	VX; tabun	S: high sensitivity; using a portable device; W: relatively high cost; require extensive sample pre-treatment;	LOD: ~13 fmol (VX); ~670 fmol (tabun) [2]
SERS	DMMP ; PMP; DEPA; CEES	S: enormous electro-magnetic enhancement; W: relatively high cost; require extensive sample pre-treatment;	LOD: lower than 1 ppm; [3]
SERS	VX and its hydroly sis product s	S: could distinguish the nerve agent VX and its hydrolysis products; W: relatively high cost; require extensive sample pre-treatment;	50-100ug L ⁻¹ [4]
CIEE/FS	DCP	S: high sensitivity; large emission shift; W: time-consuming; require extensive sample pre-treatment; relying on sophisticated instruments	LOD: 17 nmol L ⁻¹ [5]
HPLC- MS/CE- UV	DMT; DET; DPT; DIT	S: sufficient separation of these four compounds in environmental forensic analysis of samples with minimum sample pre-treatment; W: time-consuming; require extensive sample pre-treatment; relying on	LOD: 0.015-0.025mg L ⁻¹ (HPLC-MS); 1.5-2mg L ⁻¹ (CE-UV) [6]

		sophisticated instruments	
		S: could detect real samples; good alternative extraction method;	LOD: 0.2 ng L ⁻¹
SPME/GC	TnBP;	W: time-consuming;	(TnBP); 1.5ng L ⁻¹ [7]
-MS	TEHP	require extensive sample pre-treatment; relying on sophisticated instruments	¹ (TEHP)
		S: realized qualitative and quantitative determination of pesticide residues in mangoes;	LOD: 1.0-3.3 [8]
SPME/GC	14 pesticide residue	W: time-consuming;	$\mu\text{g kg}^{-1}$
-MS	s	require extensive sample pre-treatment; relying on sophisticated instruments	
		S: gas detection; short detection time (2.8s)	
IMS/DMS	Tabun, Sarin, Soman, VX	W: time-consuming; require extensive sample pre-treatment; relying on sophisticated instruments	LOD: 20 $\mu\text{g m}^{-3}$ [9]
		S: could detect sample in a variety of sample matrixes (water, kerosene, gasoline, diesel);	LOD: lower than [10]
IM(tof)MS	DMMP	W: time-consuming; require extensive sample pre-treatment; relying on sophisticated instruments	1000 ppm;

Abbreviation: surface-enhanced Raman scattering (SERS); dimethyl methylphosphate (DMMP); pinacolyl methylphosphonate (PMP); diethyl phosphoramidate (DEPA); chloroethyl ethylsulfide (CEES); cyclization-induced emission enhancement (CIEE); fluorescence spectrum (FS); diethyl chlorophosphate (DCP); high-performance liquid

chromatography-mass spectrometry (HPLC-MS); capillary electrophoresis with direct ultraviolet detection (CE-UV); N, N-(dialkyl)aminoethanesulfonicacids, where alkyl = methyl, ethyl, n-propyl or iso-propyl (DMT, DET, DPT, and DIT, re-spectively); solid-phase microextraction (SPME); gas chromatography–mass spectrometry (GC–MS); tri-n-butyl phosphate (TnBP); tris (2-ethylhexyl) phosphate (TEHP); ion mobility spectrometry (IMS); differential mobility spectrometry (DMS); ion mobility orthogonal reflector time-of-flight mass spectrometer (IM-(tof)MS);

References:

- [1] C. X. Yan, F. L. Qi, S. G. Li, J. Y. Xu, C. Liu, Z. H. Meng, L. L. Qiu, M. Xue, W. Lu and Z. Q. Yan, *Talanta*, 2016, 159, 412-417.
- [2] A. Hakonen, T. Rindzevicius, M.S. Schmidt, P.O. Andersson, L. Juhlin, M. Svedendahl, A. Boisen, M. Kall, Detection of nerve gases using surface-enhanced Raman scattering substrates with high droplet adhesion, *Nanoscale* 8 (2016) 1305-1308.
- [3] F. Yan, T. Vo-Dinh, Surface-enhanced Raman scattering detection of chemical and biological agents using a portable Raman integrated tunable sensor, *Sensor. Actuat. B-Chem.* 121 (2007) 61-66.
- [4] S. Farquharson, A. Gift, P. Maksymiuk, F. Inscore, Surface-enhanced Raman spectra of VX and its hydrolysis products, *Appl. Spectrosc.* 59 (2005) 654-660.
- [5] A.K. Mahapatra, K. Maiti, S.K. Manna, R. Maji, S. Mondal, C. Das Mukhopadhyay, P. Sahoo, D. Mandal, A cyclization-induced emission enhancement (CIEE)-based ratiometric fluorogenic and chromogenic probe for the facile detection of a nerve agent simulant DCP, *Chem. Commun.* 51 (2015) 9729-9732.
- [6] I. Rodin, A. Stavrianidi, R. Smirnov, A. Braun, O. Shpigun, I. Rybalchenko, New Techniques for Nerve Agent Oxidation Products Determination in Environmental Water by High-Performance Liquid Chromatography-Mass Spectrometry (HPLC-MS) and Capillary Electrophoresis (CE) with Direct Ultraviolet (UV) Detection, *Environ. Forensics* 14 (2013) 87-96.
- [7] Y.C. Tsao, Y.C. Wang, S.F. Wu, W.H. Ding, Microwave-assisted headspace solid-phase microextraction for the rapid determination of organophosphate esters in aqueous samples by gas chromatography-mass spectrometry, *Talanta* 84 (2011) 406-410.
- [8] A. Menezes Filho, F.N. dos Santos, P.A. de Paula Pereira, Development, validation and application of a methodology based on solid-phase micro extraction

followed by gas chromatography coupled to mass spectrometry (SPME/GC-MS) for the determination of pesticide residues in mangoes, *Talanta* 81 (2010) 346-354.

[9] M. Maziejuk, M. Ceremuga, M. Szyposzynska, T. Sikora, A. Zalewska, Identification of organophosphate nerve agents by the DMS detector, *Sensor. Actuat. B-Chem.* 213 (2015) 368-374.

[10] W.E. Steiner, S.J. Klopsch, W.A. English, B.H. Clowers, H.H. Hill, Detection of a chemical warfare agent simulant in various aerosol matrixes by ion mobility time-of-flight mass spectrometry, *Anal. Chem.* 77 (2005) 4792-4799.

6. Calculated wavelength of 2D-PC

6.1 The 2D Bragg diffraction equation.

The diffraction process of 2D-PC was illustrated in figure S3, while white source (S1, S2) illuminated below the sample at an incidence angle of 45° (θ), and the structural color was recorded above the sample along the normal.

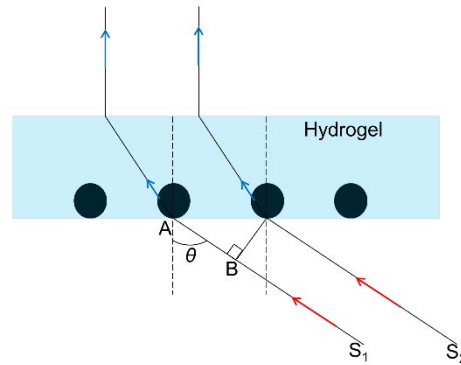


Figure S3 Illustration of the diffraction process of 2D-PC

The path difference Δ was given by

$$\Delta = n_{air}(AB) = n_{air}(p \sin \theta) = p \sin \theta = \frac{\sqrt{3}}{2} d \sin \theta \quad (S2)$$

Where n_{air} is the refractive index of air ($n_{air}=1$), p is the distance between adjacent lattice rows. θ is the incidence angle. According to reference¹, p is relate to the lattice spacing (d) by

$$p = \frac{\sqrt{3}}{2} d \quad (S3)$$

According to Bragg's law, while the path difference (Δ) is equal to a whole number of wavelengths, the diffraction will be strengthened. So the path difference meets following equation:

$$\frac{\sqrt{3}}{2} d \sin \theta = m \lambda \quad (S4)$$

Where m is the diffraction order, λ is the diffracted wavelength. While the incidence angle was fixed, and we surmise the diffraction was the first-order diffraction. According to the determination of particle spacing, we can also calculate the diffracted wavelength of 2D-PC in different condition.

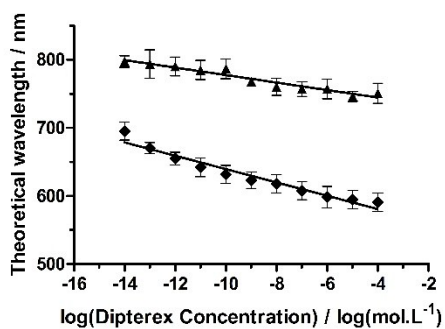


Figure S4 AChE-functionalized 2D-PC (◆) and unfunctionalized 2D-PC (▲) for dipterex detection.